1-1-2013

A multi-objective optimal PID control for a nonlinear system with time delay

Furui Xiong

Zhichang Qin

Carlos Hernández

Yousef Sardahi

Yousef Narajani

See next page for additional authors

Authors
Furui Xiong, Zhichang Qin, Carlos Hernández, Yousef Sardahi, Yousef Narajani, Wei Liang, Yang Xue, Oliver Schütze, and Jianqiao Sun

A multi-objective optimal PID control for a nonlinear system with time delay

Furui Xiong,[1] Zhichang Qin,[1] Carlos Hernández,[2] Yousef Sardahi,[3] Yousef Narajani,[3] Wei Liang,[3] Yang Xue,[1] Oliver Schütze,[2] and Jianqiao Sun[3, a)]

[1)] *Department of Mechanics, Tianjin University, Tianjin 300072, China*
[2)] *CINVESTAV-IPN, Depto de Computacion, Mexico City 07360, Mexico*
[3)] *University of California at Merced, Merced, CA 95343, USA*

(Received 2 September 2013; accepted 6 October 2013; published online 10 November 2013)

Abstract It is generally difficult to design feedback controls of nonlinear systems with time delay to meet time domain specifications such as rise time, overshoot, and tracking error. Furthermore, these time domain specifications tend to be conflicting to each other to make the control design even more challenging. This paper presents a cell mapping method for multi-objective optimal feedback control design in time domain for a nonlinear Duffing system with time delay. We first review the multi-objective optimization problem and its formulation for control design. We then introduce the cell mapping method and a hybrid algorithm for global optimal solutions. Numerical simulations of the PID control are presented to show the features of the multi-objective optimal design. [doi:10.1063/2.1306306]

Keywords delayed control system, multi-objective optimal design, cell mapping method, hybrid algorithm, Pareto optimal

The history of proportional-integral-derivative (PID) control can be traced to the 1930s. Because of vast applications of PID controls in industries, there have been many studies to develop design or tuning techniques of the control. Two classic designs are a heuristic tuning method due to Ziegler and Nichols[1] and the Smith predictor due to Smith.[2] Because feedback controls inherently are designed to meet multiple and often conflicting performance goals, comprehensive studies are usually carried out to tune control gains in order to achieve best performance.[3,4]

To achieve multiple optimized objectives in PID controlled systems, one has to make the trade-off among several conflicting performance objectives such as overshoot, peak time, settling time and tracking error.[5] For the last three decades, there have been a large number of publications on multi-objective optimal design of PID controllers. Different from the traditional single objective optimization problems (SOPs), the multi-objective optimization problems (MOPs) do not have unique solutions consisting of a single point in the design space, but rather a set, called the Pareto set. The corresponding objective function values are called the Pareto front.

Many algorithms for obtaining the Pareto set and Pareto front of MOPs have been developed. There are biologically inspired optimization algorithms such as genetic algorithm,[6] ant colony optimization,[7] immune algorithm,[8] and particle swarm optimization.[9] All these methods have been successfully applied to tune PID controls to meet multiple control objectives. Fliege and Svaiter[10] have developed several gradient-based algorithms by converting MOP to SOP for point-wise evolution and step length determination of the steepest descend search for MOP solutions. Bosman[11] expands the concept of gradient by introducing novel geometric transformations and combines the genetic algorithm for MOP searching. A gradient-free approach is introduced by Zhong et al.[12] to address undifferentiable MOPs. In the work of Custodio et al.,[13] ideas from pattern searching are adapted to direct gradient-free search. Despite the fast computational speed of the gradient-free algorithm, it is still lack of rigorous mathematical proof of its global convergence. Nevertheless, the gradient-free algorithm is effective obtaining relatively coarse Pareto sets.

Another approach to approximate the Pareto set is to use the set oriented methods with subdivision techniques.[14–16] The advantage of the set oriented methods is that they generate an approximation of the global Pareto set in one single run of the algorithm. Further, they are applicable to a wide range of optimization problems and are characterized by a great robustness. The cell mapping method in this study is the predecessor of the set oriented methods, and was proposed by Hsu[17] for global analysis of nonlinear dynamical systems. In the cell mapping method for MOPs, the dynamical systems are derived from multi-objective optimization search algorithms. Lately, we have found that the simple cell mapping (SCM) method can obtain the global optimal solution in a quite effective manner for low and moderate dimensional problems. This paper presents a variant of the SCM method that hybridizes gradient based and gradient free optimization techniques for MOP design of delayed PID controls.

Two cell mapping methods have been extensively studied, namely, the SCM and the generalized cell mapping (GCM) to study the global dynamics of nonlinear systems.[17,18] The cell mapping methods have been applied to optimal control problems of deterministic and

[a)] Corresponding author. Email: jqsun@ucmerced.edu.

stochastic dynamic systems.[19–21] Other interesting applications of the cell mapping methods include optimal space craft momentum unloading,[22] single and multiple manipulators of robots,[23] optimum trajectory planning in robotic systems,[24] tracking control of the read-write head of computer hard disks,[25] and airfoil flutter analysis.[26] Crespo and Sun[27,28] studied the fixed final state optimal control problems with the simple cell mapping method, and applied the cell mapping methods to the optimal control of dynamical systems described by Bellman's principle of optimality.[29] The application of the SCM method to MOPs represents a new application domain of the cell mapping methods.

In this paper, we demonstrate the SCM method for MOPs by studying a multi-objective optimal delayed PID control of a Duffing system. Such a control problem has not been studied before to our best knowledge.

Consider a second order nonlinear dynamical system with time delays given by

$$\begin{aligned}\dot{x}_1 &= x_2,\\ \dot{x}_2 &= f\left(x_1, x_2, x_1\left(t-\tau_{\mathrm{s}}\right), x_2\left(t-\tau_{\mathrm{s}}\right)\right) + \\ &\quad u\left(t-\tau_{\mathrm{c}}\right),\end{aligned} \tag{1}$$

where f is a nonlinear function of its arguments such that the solution of the differential equation exists. τ_{s} is a system delay, and τ_{c} is a control delay. For more information about time delay, the reader is referred to the book by Insperger and Stepan.[30] We consider a PID feedback control given by

$$\begin{aligned}u(t) = k_{\mathrm{p}}\left(r(t)-x_1(t)\right) + k_{\mathrm{i}}\int_0^t \left(r(\hat{t})-x_1(\hat{t})\right)\,\mathrm{d}\hat{t} - \\ k_{\mathrm{d}}x_2(t),\end{aligned} \tag{2}$$

where $r(t)$ is a reference input, k_{p}, k_{i}, and k_{d} are the PID control gains. We introduce a third state variable x_3 such that $\dot{x}_3(t) = r(t) - x_1(t)$. The extended system is governed by the following equations.

$$\begin{aligned}\dot{x}_1 &= x_2,\\ \dot{x}_2 &= f\left(x_1, x_2, x_1\left(t-\tau_{\mathrm{s}}\right), x_2\left(t-\tau_{\mathrm{s}}\right)\right) + u\left(t-\tau_{\mathrm{c}}\right),\\ \dot{x}_3 &= r(t) - x_1(t),\end{aligned} \tag{3}$$

where

$$u(t) = k_{\mathrm{p}}\left(r(t)-x_1(t)\right) + k_{\mathrm{i}}x_3 - k_{\mathrm{d}}x_2(t). \tag{4}$$

Assume that the closed-loop system is stable and $r(t)$ is a step function. In steady-state, we have a unique equilibrium solution,

$$x_1^* = 1,\quad x_2^* = 0,\quad x_3^* = -\frac{1}{k_{\mathrm{i}}}f(1,0,1,0). \tag{5}$$

It should be pointed out that the uncontrolled nonlinear system may have multiple equilibrium solutions. The stability of the steady state response can be analyzed by linearizing the system. Let $\boldsymbol{z} = [z_1, z_2, z_3]^{\mathrm{T}}$ be the perturbation of the system away from the steady state $\boldsymbol{x}^* = [x_1^*, x_2^*, x_3^*]^{\mathrm{T}}$. We have

$$\dot{\boldsymbol{z}}(t) = \boldsymbol{A}\boldsymbol{z}(t) + \boldsymbol{A}_{\mathrm{s}}\boldsymbol{z}\left(t-\tau_{\mathrm{s}}\right) + \boldsymbol{A}_{\mathrm{c}}\boldsymbol{z}\left(t-\tau_{\mathrm{c}}\right), \tag{6}$$

where $\boldsymbol{A}$, $\boldsymbol{A}_{\mathrm{s}}$, $\boldsymbol{A}_{\mathrm{c}}$ are matrices of the linearized system and are functions of the control gains. The stability of the linearized system can be analyzed by the method of continuous time approximation.[31,32]

A MOP can be expressed as

$$\min_{\boldsymbol{k}\in Q}\{\boldsymbol{F}(\boldsymbol{k})\}, \tag{7}$$

where $\boldsymbol{F}$ is the map that consists of the objective functions $f_i : Q \to \mathbf{R}^1$ under consideration.

$$\boldsymbol{F} : Q \to \mathbf{R}^k,\ \boldsymbol{F}(\boldsymbol{k}) = [f_1(\boldsymbol{k}), f_2(\boldsymbol{k}), \ldots, f_k(\boldsymbol{k})]. \tag{8}$$

$\boldsymbol{k} \in Q$ is a q-dimensional vector of design parameters. The domain $Q \subset \mathbf{R}^q$ can in general be expressed by inequality and equality constraints

$$\begin{aligned}Q = \{&\boldsymbol{k}\in\mathbf{R}^q \mid g_i(\boldsymbol{k}) \leqslant 0,\\ &i = 1,2,\ldots,l;\ h_j(\boldsymbol{k}) = 0,\ j = 1,2,\ldots,m\}.\end{aligned} \tag{9}$$

Next, we define optimal solutions of the MOP by using the concept of dominance.[33]

Definition 1

(a) Let $\boldsymbol{V}, \boldsymbol{W} \in \mathbf{R}^k$. The vector $\boldsymbol{V}$ is said to be less than $\boldsymbol{W}$ (in short: $\boldsymbol{V} <_p \boldsymbol{W}$), if $V_i < W_i$ for all $i \in \{1, 2, \ldots, k\}$. The relation $\leqslant_p$ is defined analogously.

(b) A vector $\boldsymbol{v} \in Q$ is said to be dominated by a vector $\boldsymbol{w} \in Q$ ($\boldsymbol{w} \prec \boldsymbol{v}$) with respect to the MOP (7) if $\boldsymbol{F}(\boldsymbol{w}) \leqslant_p \boldsymbol{F}(\boldsymbol{v})$ and $\boldsymbol{F}(\boldsymbol{w}) \neq \boldsymbol{F}(\boldsymbol{v})$, else $\boldsymbol{v}$ is said to be non-dominated by $\boldsymbol{w}$.

If a vector $\boldsymbol{w}$ dominates a vector $\boldsymbol{v}$, then $\boldsymbol{w}$ can be considered to be a "better" solution of the MOP. The definition of optimality or the "best" solution of the MOP is now straightforward.

Definition 2

(a) A point $\boldsymbol{w} \in Q$ is called Pareto optimal or a Pareto point of the MOP (7) if there is no $\boldsymbol{v} \in Q$ which dominates $\boldsymbol{w}$.

(b) The set of all Pareto optimal solutions is called the Pareto set denoted as

$$\mathcal{P} := \{\boldsymbol{w} \in Q : \boldsymbol{w} \text{ is a Pareto point of the MOP(7)}\}. \tag{10}$$

(c) The image $\boldsymbol{F}(\mathcal{P})$ of $\mathcal{P}$ is called the Pareto front.

The Pareto front typically forms $(k-1)$-dimensional manifolds under certain mild assumptions on the MOP.[34] Recent studies with the SCM method seem to suggest that the Pareto front may have fine structures for MOPs of complex dynamical systems.

Multi-objective optimal design

As an example of MOPs, we consider the multi-objective optimal control design with the gains $\boldsymbol{k} = [k_{\mathrm{p}}, k_{\mathrm{i}}, k_{\mathrm{d}}]^{\mathrm{T}}$ as design parameters for the system discussed previously. Peak time and overshoot are common objectives in time domain control design.[6,35,36] We consider the MOP for the optimal control gain $\boldsymbol{k}$ to minimize the following three objectives

$$\min_{\boldsymbol{k}\in Q}\{t_{\mathrm{p}}, M_{\mathrm{p}}, e_{\mathrm{IAE}}\} \text{ subject to the stability of system (6)}, \tag{11}$$

where M_{p} stands for the overshoot of the response to a step reference input, t_{p} is the corresponding peak time and e_{IAE} is the integrated absolute tracking error

$$e_{\mathrm{IAE}} = \int_0^{T_{\mathrm{ss}}} \left|r(\hat{t}) - x_1(\hat{t})\right| \,\mathrm{d}\hat{t}, \tag{12}$$

where $r(t)$ is a reference input and T_{ss} is the time when the response is close to be in the steady state. The closed-loop response of the system for each design trial can be computed with the help of numerical integration programs of delayed differential equations.

The cell mapping methods describe system dynamics with cell-to-cell mappings by discretizing both the phase space and time. In MOPs, the SCM method is applied to the dynamic search process in the design parameter space, not to the original dynamical system in time domain. The point-to-point mapping obtained from the gradient search algorithm for MOPs can be written as

$$\boldsymbol{k}(i) = \boldsymbol{G}(\boldsymbol{k}(i-1)), \tag{13}$$

where $\boldsymbol{k}\,(i) \in \mathbf{R}^q$ is the design vector at the i-th mapping step. In the SCM, the dynamics of an entire cell denoted as Z is represented by the dynamics of its center. The center of Z is mapped according to the point-to-point mapping. The cell that contains the image point is called the image cell of Z. The cell-to-cell mapping corresponding to Eq. (13) is denoted by C,

$$Z(i) = C(Z(i-1)). \tag{14}$$

To illustrate how the SCM is constructed for MOPs, we present a directed search (DS) algorithm,[37,38] which has the benefit of needing less information to perform the local search for mininum, assuming that the parameter space Q is discretized into a collection of finite size cells and that the SCM method is applied.

The first step of the SCM method for MOP is to compute the objective functions at the center point of all the cells in Q. The DS algorithm allows to steer the search into any pre-selected direction $\boldsymbol{d} \in \mathbf{R}^k$ in the objective space. $\boldsymbol{d}$ is usually chosen from the current location in the objective function space to point to a direction along which all the objective functions decrease.[39] To apply the gradient free version of this algorithm within SCM, we can proceed as follows: Choose $r \geqslant q$ neighboring cells of a current cell under processing. Define unit vectors as

$$\boldsymbol{\nu}_i = \frac{\boldsymbol{k}_i - \boldsymbol{k}_0}{\|\boldsymbol{k}_i - \boldsymbol{k}_0\|_2}, \quad i = 1, 2, \cdots, r, \tag{15}$$

where $\boldsymbol{k}_0$ is the center of the current cell, and $\boldsymbol{k}_i$ is the center of the i-th cell in the immediate neighborhood of $\boldsymbol{k}_0$. Define a matrix $\mathcal{F} = \{m_{i,j}\} \in \mathbf{R}^{k\times r}$ as

$$m_{i,j} = \frac{f_i(\boldsymbol{k}_j) - f_i(\boldsymbol{k}_0)}{\|\boldsymbol{k}_j - \boldsymbol{k}_0\|_2}, \tag{16}$$

which is an approximation of the directional derivative of $f_i(\boldsymbol{k}_0)$ in direction $\boldsymbol{\nu}_j$ at $\boldsymbol{k}_0$. Compute

$$\boldsymbol{\lambda} = \mathcal{F}^+\boldsymbol{d}, \tag{17}$$

where $\mathcal{F}^+$ denotes the pseudo inverse of $\mathcal{F}$.[40] Then a line search in the parameter space along the direction

$$\boldsymbol{\nu} = \sum_{i=1}^{r} \lambda_i \boldsymbol{\nu}_i, \tag{18}$$

leads to a movement along $\boldsymbol{d}$-direction in the objective space. If the search along $\boldsymbol{\nu}$-direction near the neighborhood of the current cell $\boldsymbol{k}_0$ ends at a cell $\boldsymbol{k}_{\mathrm{d}}$ which dominates $\boldsymbol{k}_0$, i.e., $\boldsymbol{F}(\boldsymbol{k}_{\mathrm{d}}) \leqslant_p \boldsymbol{F}(\boldsymbol{k}_0)$, $\boldsymbol{k}_{\mathrm{d}}$ is taken as the image cell of $\boldsymbol{k}_0$. If no such a cell can be found, the current cell $\boldsymbol{k}_0$ may be on the Pareto set, and we assign its image as itself. This is how the simple cell mappings are constructed for all the cells in the parameter space Q. After all the cells are processed, we apply the sorting algorithm due to Hsu[17] to identify periodic and transient cells in the discretized domain Q. The periodic cells represent an approximation of the Pareto set, with possibly one exception.

If no transient cells are mapped to a periodic cell with period one, the periodic cell is isolated. We change it to be the sink cell. This can happen when a cell is not on the Pareto set and none of its neighboring cells dominates it.

Next, we discuss a hybrid algorithm for computing the SCM of a MOP. The hybrid algorithm consists of a gradient free search on a relatively coarse cell space and a gradient based search on the region of the approximate Pareto set obtained by the gradient free search with much refined cells. For the gradient free search, the image of a cell is selected by comparing the objective function values of all its neighboring cells. If there is only one dominant cell in the neighborhood, it becomes the image of the cell under consideration. If there are more than one dominant cells, we select the one that has the highest objective function value decrease per unit distance. Such a choice mimics the steepest gradient decent algorithm. The outcome of the gradient free search on a coarse cell partition is a covering set of the Pareto set.

We point out that gradient based approaches could be realized efficiently in the context of SCM. If the cells are small enough, one could, for instance, use the center points of the neighboring cells to obtain a finite difference approximation of the gradient at a given cell. This would in principle open the door for the usage of all gradient based search algorithms, but without explicitly computing the gradient. Since the function values for the center points of neighboring cells in all q directions are already known, the approximation of the gradient comes for free in terms of the additional function evaluations. This is the reason that a gradient search algorithm is proposed for the second step of the hybrid algorithm over the refined cell space.

Before the refinement step in the hybrid algorithm, we programmatically make the covering set larger than the collection of all periodic cells by including their immediate neighboring cells. This is a strategy to avoid the missing segments of the Pareto set. As a final step, the dominance of the cells in the Pareto set is checked in order to remove the additional cells that are brought in to avoid the missing segments of the Pareto set.

We should note that the exact image of the center of a cell is approximated by the center of its image cell. This approximation can cause significant errors in the long term solution of dynamical systems.[19,20,24] The cell mapping with a finite number of cells in the computational domain will eventually lead to closed groups of cells of the period same as the number of cells in the group. The periodic cells represent invariant sets, which can be periodic motion and stable attractors of underlying dynamical systems, and which represent the Pareto set in the context of MOPs. The rest of the cells form the domains of attraction of the invariant sets. For more discussions on the cell mapping methods, their properties and computational algorithms, the reader is referred to the book by Hsu.[17]

Consider a Duffing system such that

$$f\left(x_1, x_2, x_1\left(t-\tau_{\mathrm{s}}\right), x_2\left(t-\tau_{\mathrm{s}}\right)\right) = -ax_1 - bx_1^3 - cx_2, \quad (19)$$

where $a = -1$, $b = 0.25$, and $c = 0.01$. Note that the system at the origin of the state space is unstable. The control time delay is 0.05 s. The system is under the delayed PID control in Eq. (4). We study the MOP defined in Eq. (11) to design the control gain $\boldsymbol{k}$. The time-domain response of the Duffing system for each selection of the control gain is generated with the delayed differential equation integration algorithm (dde23) in Matlab. The integrated absolute tracking error e_{IAE} is calculated over time with $T_{\mathrm{ss}} = 4$ s. The design space for the parameters is chosen as

$$Q = \{\boldsymbol{k} \in [80, 120] \times [10, 30] \times [10, 30] \subset \mathbf{R}^3\}. \quad (20)$$

We impose the constraints

$$[t_{\mathrm{p}}, M_{\mathrm{p}}, e_{\mathrm{IAE}}, \lambda_{\mathrm{ss}}] \leqslant [2.5, 6\%, 0.75, -0.25], \quad (21)$$

where λ_{ss} denotes the largest real part of the eigenvalues of the linearized steady-state system (6). The eigenvalues of the linearized system are computed with the method of continuous time approximation and the Chebyshev interpolation.[31,32] The constraint on the eigenvalues is intended to provide the stability robustness of the optimized control system. Since the original system is nonlinear, the stability condition should be imposed on the steady-state equilibrium solutions.

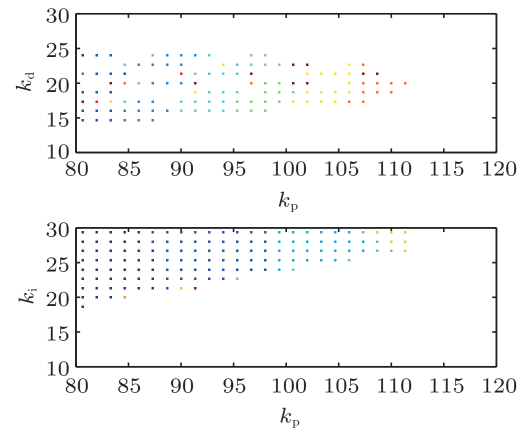

Fig. 1. The Pareto set obtained on the rough grid by the SCM method for the Duffing system with delayed control. The color code indicates the level of the other design variable. Red denotes the highest value, and dark blue denotes the smallest value.

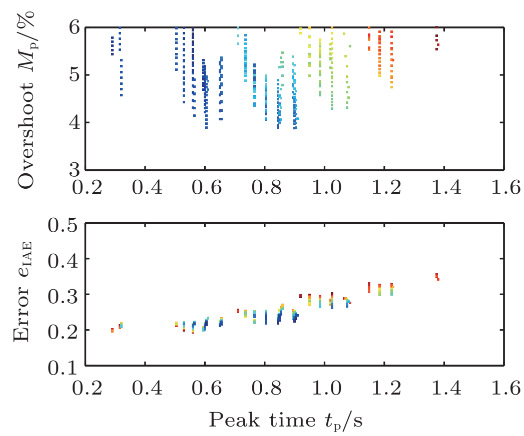

Fig. 2. The Pareto front of the Duffing system corresponding to the Pareto set in Fig. 1. The color code indicates the level of the other objective function. Red denotes the highest value, and dark blue denotes the smallest value.

Initially, we select the number of divisions of the three control gain space as $\boldsymbol{N} = [30, 15, 15]$. The cells of the rough Pareto set is sub-divided into 27 cells ($3 \times 3 \times 3$). The first run of the SCM method on the rough grid finds 460 cells representing the Pareto set shown in Fig. 1. The corresponding Pareto front is shown in Fig. 2. The CPU time of the first run is 1 382.4 s. The second run on the sub-divided cells finds the Pareto set with 2 386 cells shown in Fig. 3. The refined Pareto front is shown in Fig. 4. The CPU time of the second run is 5 695.5 s.

We should point out that the Pareto fronts obtained by the SCM method have fine global structures. Such fine structures of Pareto fronts are not often found in the literature before. Finally, we present an example of step response under the delayed control with the gain $[k_{\mathrm{p}}, k_{\mathrm{i}}, k_{\mathrm{d}}] = [82.444\,4, 21.777\,8, 14.222\,2]$. The result is shown in Fig. 5. The step response shows excel-

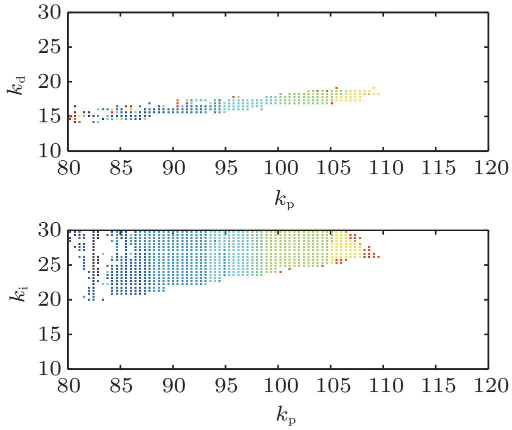

Fig. 3. The refined Pareto set shown in Fig. 1 of the Duffing system with delayed control by the SCM method. The color code indicates the level of the other design variable. Red denotes the highest value, and dark blue denotes the smallest value.

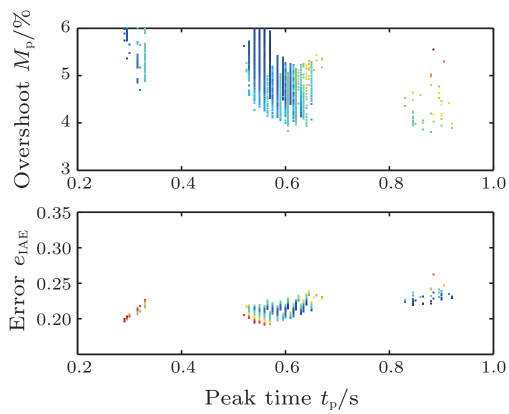

Fig. 4. The refined Pareto front of the Duffing system corresponding to the Pareto set in Fig. 3. The color code indicates the level of the other objective function. Red denotes the highest value, and dark blue denotes the smallest value.

lent time-domain performance with $[t_p, M_p, e_{IAE}, \lambda_{ss}] = [0.330\,0, 0.048\,829, 0.215\,5, -0.278\,1]$.

We have presented a multi-objective PID control design for the Duffing system by using the SCM method. The time-domain specifications of the step response are used as the objective functions. A constraint on the closed-loop eigenvalue of the linearized system about the steady-state equilibrium solution is also imposed that provides the stability robustness of the optimized PID controls. The SCM method is implemented in a hybrid manner as described earlier. We have found that the hybrid algorithm for the SCM method delivers substantial computational savings while obtaining comparably accurate solutions for the Pareto set and Pareto front.

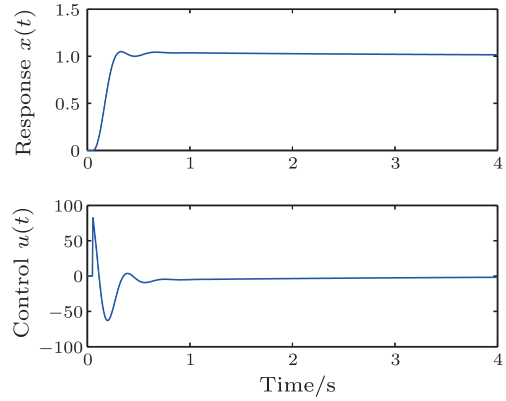

Fig. 5. An example of the step response of the Duffing system under the delayed PID control with $[k_p, k_i, k_d] = [82.444\,4, 21.777\,8, 14.222\,2]$.

This work was supported by the UC MEXUS-CONACyT ("Cell-to-cell Mapping for Global Multi-objective Optimization"), the National Natural Science Foundation of China (11172197), and the Natural Science Foundation of Tianjin through a key-project grant. Carlos Hernández also acknowledges support from CONACyT through a scholarship to pursue graduate studies at the Computer Science Department of CINVESTAV-IPN.

1. J. G. Ziegler and N. B. Nichols, Journal of Dynamic Systems, Measurement and Control **115**, 220 (1942).
2. O. J. M. Smith, ISA Journal **6**, 28 (1959).
3. P. Cominos and N. Munro, IEE Proceedings-Control Theory and Applications **149**, 46 (2002).
4. Q. G. Wang, T. H. Lee, H. W. Fung, et al., IEEE Transactions on Control Systems Technology **7**, 457 (1999).
5. C. A. Kumar and N. K. Nair, in Proceedings of International Conference on Signal Processing, Communication, Computing and Networking Technologies (Piscataway, New Jersey, 2011) 424.
6. S. Panda, International Journal of Electrical Power & Energy Systems **33**, 1296 (2011).
7. I. Chiha, N. Liouane, and P. Borne, Applied Computational Intelligence and Soft Computing **2012**, 536326 (2012).
8. M. Khoie, K. Salahshoor, E. Nouri, et al., *Lecture Notes in Computer Science-Advanced Intelligent Computing Theories and Applications*, (Springer Verlag, Berlin, 2012) **6839**, 267.
9. M. I. Solihin, L. F. Tack, and M. L. Kean, International Journal on Advanced Science, Engineering and Information Technology **1**, 458 (2011).
10. J. Fliege and B. F. Svaiter, Mathematical Methods of Operations Research **51**, 479 (2000).
11. P. A. N. Bosman, IEEE Transaction on Evolutionary Computation **16**, 51 (2012).
12. X. Zhong, W. Fan, J. Lin, et al., Proceedings of the 1st IEEE International Conference on Progress in Informatics and Computing **1**, 24 (2010).
13. A. L. Custodio, J. F. A. Madeira, A. I. F. Vaz, et al., SIAM Journal on Optimization **21**, 1109 (2011).
14. M. Dellnitz, O. Schtze, and T. Hestermeyer, Journal of Optimization Theory and Applications **124**, 113 (2005).
15. J. Jahn, Computational Optimization and Applications **35**, 161 (2006).
16. O. Schütze, M. Vasile, O. Junge, et al., Engineering Optimization **41**, 155 (2009).
17. C. S. Hsu, *Cell-to-Cell Mapping, A Method of Global Analysis for Nonlinear Systems* (Springer-Verlag, New York, 1987).
18. C. S. Hsu, Journal of Applied Mechanics **47**, 931 (1980).

19. C. S. Hsu, Journal of Optimization Theory and Applications **46**, 547 (1985).
20. F. H. Bursal and C. S. Hsu, International Journal of Control **49**, 1505 (1989).
21. L. G. Crespo and J. Q. Sun, Automatica **39**, 2109 (2003).
22. H. Flashner and T. F. Burns, Journal of Guidance, Control and Dynamics **13**, 89 (1990).
23. W. H. Zhu and M. C. Leu, Proceedings of IEEE International Conference on Robotics and Automation, 1730 (1990).
24. F. Y. Wang and P. J. A. Lever, Robotics and Autonomous Systems **12**, 15 (1994).
25. J. Y. Yen, W. C. Chao, and S. S. Lu, *Computer disk file track accessing controller design based upon cell-to-cell mapping*, Proceedings of the American Control Conference, Chicago (1992).
26. Q. Ding, J. E. Cooper, and A. Y. T. Leung, Journal of Fluids and Structures **20**, 35 (2005).
27. L. G. Crespo and J. Q. Sun, Nonlinear Dynamics **23**, 391 (2000).
28. L. G. Crespo and J. Q. Sun, Journal of Guidance and Control **24**, 1029 (2000).
29. L. G. Crespo and J. Q. Sun, Nonlinear Dynamics **31**, 119 (2003).
30. T. Insperger and G. Stepan, *Semi-discretization for Time-delay Systems* (Springer, New York, 2011).
31. J. Q. Sun, Communications in Nonlinear Science and Numerical Simulation **14**, 998 (2008).
32. B. Song and J. Q. Sun, Journal of Vibration and Control **17**, 1173 (2011).
33. V. Pareto, *Manual of Political Economy* (The MacMillan Press, London, 1971).
34. C. Hillermeier, *Nonlinear Multiobjective Optimization: A Generalized Homotopy Approach* (Birkhäuser, Berlin, 2001).
35. G. P. Liu and S. Daley, Control Engineering Practice **7**, 821 (1999).
36. G. P. Liu and S. Daley, Control Engineering Practice **8**, 1045 (2000).
37. A. Lara, O. Schütze, and C. A. C. Coello, *EVOLVE A Bridge between Probability, Set Oriented Numerics and Evolutionary Computation*, edited by E. Tantar, A. A. Tantar, P. Bouvry, et al. (Springer-Verlag, New York, Dordreche, London, 2011) 305.
38. A. Lara, S. Alvarado, S. Salomon, et al., *EVOLVE - A Bridge between Probability, Set Oriented Numerics, and Evolutionary Computation II*, edited by O. Schütze, C. A. C. Coello, A. A. Tantar, et al., (Springer, Heidelbery, New York, Dordreche, London, 2011) 305.
39. I. Das and J. Dennis, SIAM Journal of Optimization **8**, 631 (1998).
40. J. Nocedal and S. Wright, *Numerical Optimization, Springer Series in Operations Research and Financial Engineering* (Springer, New York, 2006).